

1 **Changes in Satellite-Derived Impervious Surface Area at US Historical Climatology Network Stations**

2

3

4

5 Kevin Gallo^a and George Xian^b

6 ^aNOAA/NESDIS Center for Satellite Applications and Research, *visiting scientist* at US Geological Survey

7 Earth Observations and Science (EROS) Center, 47914 252nd Street, Sioux Falls, SD 57198-0001 USA,

8 kevin.p.gallo@noaa.gov

9 ^bUS Geological Survey, at Earth Observations and Science (EROS) Center, 47914 252nd Street, Sioux

10 Falls, SD 57198-0001 USA, xian@usgs.gov

11

12 **Submitted to: *ISPRS Journal of Photogrammetry and Remote Sensing***

13

14 **Corresponding author**

15 Kevin Gallo

16 USGS Earth Observations and Science (EROS) Center

17 47914 252nd Street, Sioux Falls, SD 57198-0001, USA

18 Email: kgallo@usgs.gov

19 Phone: +1-605-594-2748

20

21 **Keywords:** impervious surface area, land cover change, urbanization, climate station siting

22 **Changes in Satellite-Derived Impervious Surface Area at US Historical Climatology Network stations**

23

24 **ABSTRACT**

25 The difference between 30 m gridded Impervious Surface Area (ISA) between 2001 and 2011 was
26 evaluated within 100 and 1000 m radii of the locations of climate stations that comprise the US
27 Historical Climatology Network. The amount of area associated with observed increases in ISA above
28 specific thresholds was documented for the climate stations. Over 32% of the USHCN stations exhibited
29 an increase in ISA of $\geq 20\%$ between 2001 and 2011 for at least 1% of the grid cells within a 100 m radius
30 of the station. However, as the required area associated with ISA change was increased from $\geq 1\%$ to
31 $\geq 10\%$, the number of stations that were observed with a $\geq 20\%$ increase in ISA between 2001 and 2011
32 decreased to 113 (9% of stations). When the 1000 m radius associated with each station was examined,
33 over 52% (over 600) of the stations exhibited an increase in ISA of $\geq 20\%$ within at least 1% of the grid
34 cells within that radius. However, as the required area associated with ISA change was increased to
35 $\geq 10\%$ the number of stations that were observed with a $\geq 20\%$ increase in ISA between 2001 and 2011
36 decreased to 35 (less than 3% of the stations). The gridded ISA data provides an opportunity to
37 characterize the environment around climate stations with a consistently measured indicator of a
38 surface feature. Periodic evaluations of changes in the ISA near the USHCN and other networks of
39 stations are recommended to assure the local environment around the stations has not significantly
40 changed such that observations at the stations may be impacted.

41

42

43

44

45

46

47 1. INTRODUCTION

48 The impact of environmental factors (e.g., land use/land cover), and changes in these factors, on
49 observed near-surface air temperature have been the topic of numerous studies (Karl et al, 1988, Gallo
50 et al 1996, Hale et al 2006, Pielke et al 2007a, Pielke et al 2007b, Christy et al 2006, Christy et al 2009,
51 Mahmood et al 2010, Fall et al 2011). Recommendations are available for the placement of climate
52 stations that consider surrounding environmental factors (NOAA 2002, WMO 2012). However, as has
53 been pointed out (e.g., Gallo et al 1996, Fall et al 2011) even if surface air temperature stations are
54 initially placed at ideal locations, the surrounding region may develop over time and alter the
55 environment of the station and the recorded observations.

56 The influence of environmental factors on station observations, based on the station location
57 (station siting) and the surrounding environment, has been the topic of several studies. Gallo et al
58 (1996) utilized the results of a climate station-observer survey of land cover within 100, 1000, and
59 10,000 m of USHCN stations to assess the influence of land cover within these radii on diurnal
60 temperatures at the stations. Hanamean Jr. et al (2003) assessed satellite derived land cover within
61 1000 and 5000 m of station locations in an assessment of the influence of vegetation within these radii
62 on maximum and minimum temperatures. In a review that included general recommendations of urban
63 station location assessment Oke (2006) defines several environmental factors and spatial scales of
64 interest relevant to observations in urban environments. Leroy (2010) presented a classification system
65 for rating stations based on the environmental factors that potentially could influence the station
66 observations. The optimal classification for temperature observation included a recommendation that
67 the station “measurement point” may be located “at more than 100 m from heat sources or reflective
68 surfaces (buildings, concrete surfaces, car parks etc.)” The classification system presented by Leroy
69 (2010) for temperature observations are similar to those included in the WMO guidelines for
70 meteorological observations (WMO, 2012).

71

72 Impervious surface area (ISA) represents a physical characteristic of the land surface that is
73 correlated with the amount of urban-related features (e.g., asphalt, concrete, rooftops) within an
74 observed area (Arnold and Gibbons 1996). Oke (2006) recommended ISA as one of the factors that can
75 be utilized to characterize the environment of climate stations. The U.S. Geological Survey's (USGS)
76 National Land Cover Database provides impervious surface products at five year intervals beginning in
77 2001 (Homer et al., 2015). The ISA dataset was developed from Landsat data (Xian and Homer, 2010)
78 and represents the fraction of impervious surface area in a 30 m grid cell. This spatial resolution
79 facilitates evaluation of ISA within relatively close proximity to land surface structures, e.g., climate
80 stations, which may be impacted by changes in nearby ISA. The 2001 NLCD 30-m ISA dataset was utilized
81 by Elvidge et al, (2007) as a reference in their global inventory of ISA at a 1-km resolution.

82 ISA has been included in numerous studies that characterize or assess land cover changes,
83 particularly urbanization (Elvidge et al 2007, Xian et al 2007, Xian et al., 2012). An impervious surface
84 metric that relies on satellite imagery provides a uniform data source for urban land cover extent and
85 intensity. The method is useful for regional scale urban land change analysis and should be applicable to
86 other forms of urban landscape delineation, such as individual developments and neighborhoods. The
87 results from the analysis of updating impervious surface distribution in the Gulf of Mexico region reveal
88 the spatial patterns of impervious surface and urban land cover transition (Xian et al., 2012).

89 Through analysis of land use, land cover, and ISA changes and comparisons with baseline
90 information, transitions of nonurban land to urban land and urban intensifications within urban areas,
91 as well as how fast and in what areas the changes have occurred can be determined in a large area. A
92 continuous record (1984-2010) of ISA developed from Landsat data (Sexton et al 2013) was used to
93 evaluate long-term urban land cover change in the Washington, D.C.-Baltimore, MD metropolitan area.
94 Song et al (2016) utilized the data included in the Sexton et al (2013) analysis to analyze the magnitude,

95 timing, and duration of ISA change within the Washington D.C.-Baltimore, MD region. Zhang and Weng
96 (2016) utilized a time-series of Landsat data from 1988 to 2013 in an analysis of the annual dynamics of
97 ISA in the Pearl River Delta of China.

98 ISA has also been combined with gridded satellite-derived land surface temperature (Xian and
99 Crane 2006, Yuan and Bauer 2007, Zhang et al 2009, Imhoff et al 2010, Zhang et al 2010), and gridded air
100 temperatures (Gallo and Xian 2014) in studies that included spatial analyses of urban heat islands. The
101 spatial analysis of UHI using ISA and MODIS land surface temperature (LST) across the conterminous
102 United States (CONUS) suggested that urban areas are substantially warmer (2.9 °C annual average)
103 than the non-urban fringe, except for urban areas in biomes with arid and semiarid climates (Imhoff et
104 al., 2010). The analysis and observational results also show that the urban heat island amplitude both
105 increases with city size and is seasonally asymmetric for a large number of cities across most biomes.

106 The U.S. Historical Climatology Network (USHCN) temperature dataset is routinely used
107 “to quantify national- and regional-scale temperature changes in the conterminous United States”
108 (NOAA 2016). In a study of the influence of land cover on observed diurnal temperature range, Gallo et
109 al (1996), utilized the results of a climate station-observer survey of land cover within 100, 1000, and
110 10,000 m of USHCN stations. Land cover within 100 m of the climate stations resulted in the greatest
111 influence on the observed diurnal temperature range, with the influence of land cover decreasing as the
112 surveyed radii increased. Since the station observers were relied on for the determination of dominant
113 land cover classes within the various distances from the stations, there was potentially some subjectivity
114 and inconsistency introduced into the land cover determinations. The 30 m gridded USGS ISA data
115 provides an opportunity to characterize the environment around USHCN climate stations with a
116 consistently measured indicator of surface features. This updated characterization of the land surface
117 change within the vicinity of climate stations could ultimately be used to assess the influence of these
118 changes on the climate variables observed at the stations.

119 The objective of this study was to assess and document the change in ISA from 2001 to 2011 at
120 USHCN station locations across the conterminous United States using NLCD 2001 and 2011 impervious
121 surface products.

122 **2. MATERIALS and METHODS**

123 2.1 Data Sets Utilized

124 The USGS NLCD ISA product represents fractional cover of imperviousness in each 30 m grid cell.
125 Small or large ISA magnitude represent less or more imperviousness coverage and therefore the percent
126 ISA has been used to define different urban land cover categories in the NLCD land cover product. While
127 available at five year intervals (2001, 2006, and 2011) only the 2001 and 2011 ISA data sets were
128 evaluated in this study to maximize the potential difference and contrast in ISA. The ISA change product
129 was produced using an approach for updating new impervious surface growth and intensification (Xian
130 et al., 2011; Xian et al., 2012). This method is consisted of three major procedures: training data
131 refinement, creation of regression models, and change comparison. The method employed the baseline
132 year NLCD impervious surface product as the baseline estimate and Landsat imagery pairs between
133 baseline and target years as the primary data source for identifying changed areas.

134 Ancillary data including nighttime stable-light satellite imagery (NSLS) from the NOAA Defense
135 Meteorological Satellite Program (DMSP), slope, and elevation were also used to create regression tree
136 models for predicting new percent impervious surface in changed areas. Three major steps were
137 required for this process including modeling an impervious surface, comparison of model outputs, and
138 final product clean-up. In the modeling step, DMSP nighttime lights imagery in the baseline year was
139 superimposed on the NLCD impervious surface product in the same year to exclude low density
140 impervious areas outside urban and suburban centers to ensure only urban core areas be used to
141 provide a stable and reliable training dataset. Two training datasets, one having a relatively large urban
142 extent and one having a relatively small extent, were produced through imposing thresholds of

143 nighttime lights imagery on the baseline impervious product. In the comparison step, each of the two
144 training datasets combined with the baseline year Landsat imagery was separately applied with
145 regression tree algorithms to build up regression tree models (Xian and Homer, 2010).

146 Two sets of regression tree models were created and used to produce two baseline year
147 synthetic impervious surface products. Similarly, the same two training datasets were used with the
148 target year Landsat and DMSP NSLS images to create two sets of regression tree models and produce
149 two target year synthetic impervious surface products to ensure that only stable predictions are chosen
150 as intermediate products. In the cleanup step, the two synthetic product pairs were then compared to
151 remove false estimates due to strong reflectance from nonurban areas and to retain the baseline
152 impervious values in the unchanged areas. The target year impervious surface was updated individually
153 in every Landsat scene over the entire CONUS, with individual scene products subsequently mosaicked
154 together to produce a seamless target impervious surface product. To produce the NLCD 2006
155 impervious surface product, 2001 is the baseline year and 2006 is the target year. For the NLCD 2011
156 impervious surface product, the baseline and target years are 2006 and 2011.

157 In the NLCD 2011 product, additional process was implemented in addition to identifying new
158 impervious features for 2011 because the process was sensitive enough to capture many previously
159 unidentified impervious areas from earlier periods (Homer et al., 2015). It would have inaccurately
160 placed the change in the wrong period by identifying these areas as 2011 change. To correct this, an
161 intensive combination of hand editing and automated processes was implemented to identify and sort
162 potential additions into the proper NLCD period (2001, 2006, or 2011). This process was extensively
163 dependent on the use of high-resolution imagery from each period to accurately identify and sort the
164 additions captured in 2011. All other impervious features were also checked during this process,
165 enabling overall accuracy to be improved. These special edits were only focused on the eastern half of
166 CONUS because this area had the most inaccuracies from earlier periods. The additional processing

167 resulted in a much improved impervious product throughout all published years and a more consistent
168 national product.

169 While the accuracy assessment associated with the 2011 ISA dataset is still under evaluation, a
170 user accuracy (Story and Congalton, 1986) of 67% was determined for grid cell changes in ISA between
171 the 2001 and 2006 ISA datasets (Wickham et al., 2013). Additionally, a user accuracy of 99% was
172 associated with a grid cell identified as exhibiting no change in ISA between 2001 and 2006. The spatial
173 location accuracy of the Landsat data used in preparation of the ISA dataset is 30 m or less (Landsat,
174 2016).

175 The climate stations evaluated in this study included those that comprise the US Historical
176 Climatology Network (USHCN). The USHCN dataset is a subset of the NOAA Cooperative Observer
177 Program Network with locations “selected according to their spatial coverage, record length, data
178 completeness, and historical stability” (NOAA 2016). The USHCN dataset includes stations with
179 temperature records that originate in the late 1800s and early 1900s (Karl et al, 1988). The USHCN
180 station location information (version 2.5) was acquired from NOAA’s National Centers for Environmental
181 Information (formerly the National Climatic Data Center, NOAA 2016). The data retrieved included
182 station name, a station identification value, and latitude and longitude values for 1218 stations within
183 the conterminous US.

184

185 2.2 Analysis of Data

186 The 2001 and 2011 ISA data sets were acquired from the U.S. Geological Survey (USGS 2014)
187 and differences in the ISA values from 2001 to 2011 were computed. Next, the difference in ISA was
188 binned into increments of 10% into ten categories. Thus, for each grid cell, ISA differences less than 10%
189 through differences of 100% were available for analysis at 10% increments. The USHCN station location
190 information provided with the USHCN data set (Version 2.5; NOAA, 2016) was used to extract the ISA

191 differences within 100 and 1000 m of the provided station locations. The location information for the
192 USHCN stations is nominally 30 m accurate (Hausfather et al, 2013). The USHCN station location
193 information is expected to be representative of the station location; however, this information is based
194 on the location of the rain gauges at the stations and the location of the temperature sensors may vary
195 from this location. Based on a preliminary review of temperature sensor location information available
196 for 1029 of the 1281 USHCN stations (NOAA NCEI, 2016), over 90% of the temperature sensors were
197 located within 50 m of the reported station locations used in this analysis. Thus, the 100 and 1000 m
198 radii utilized in this study are appropriate for assessment of ISA at the reported station locations and the
199 location of the temperature sensors associated with the stations. The availability of accurate location
200 information for the temperature sensors at all USHCN stations is encouraged.

201 The area associated with the two radii (100 and 1000 m) from the station location was
202 intersected with the raster ISA grid (e.g., Figure 1) and the number of pixels associated with ISA change
203 for each 30 m – grid cell included in the areas was documented. A minimum of one-half the area of a
204 pixel was required to be within the intersected radii to be included in the analysis. Analysis for each
205 station included computation of the percent area that experienced an ISA change, computed as the
206 number of grid cells with an observed ISA change (e.g. $\geq 20\%$) per the minimum number of grid cells
207 potentially within the radii (100 or 1000 m). ISA changes of ≥ 10 , 20, or 50% between 2001 and 2011
208 were evaluated for the grid cells within both the 100 and 1000 m radii of each station. Station statistics
209 were additionally summarized for the entire USHCN dataset.

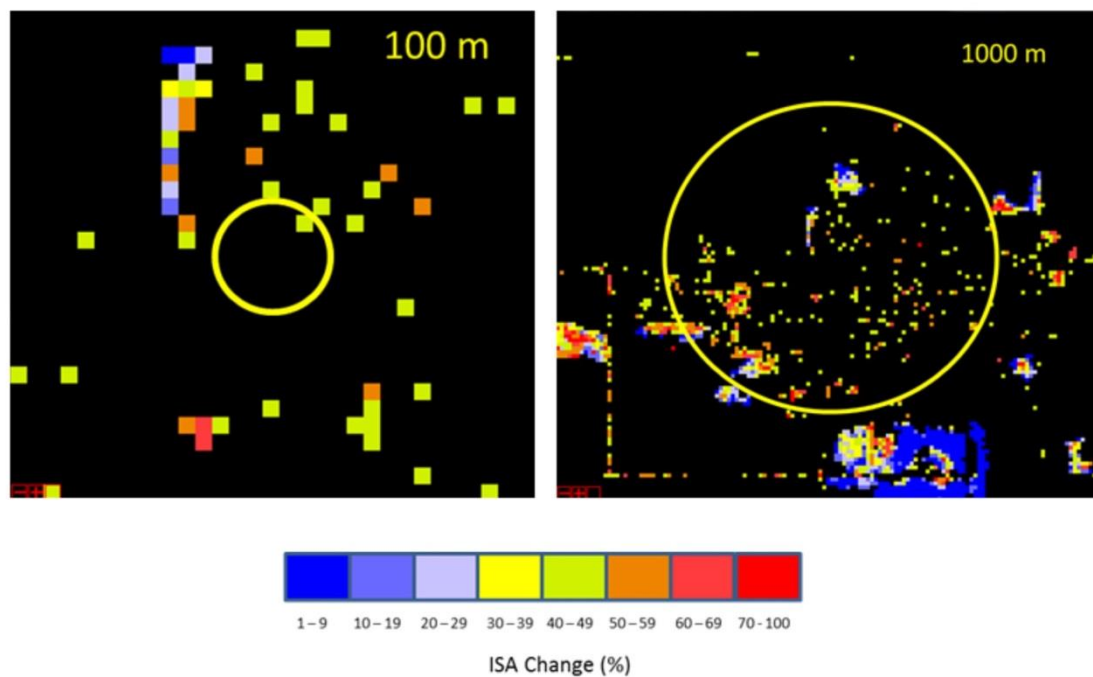
210

211

212 **3. RESULTS and DISCUSSION**

213 3.1 Local Analysis

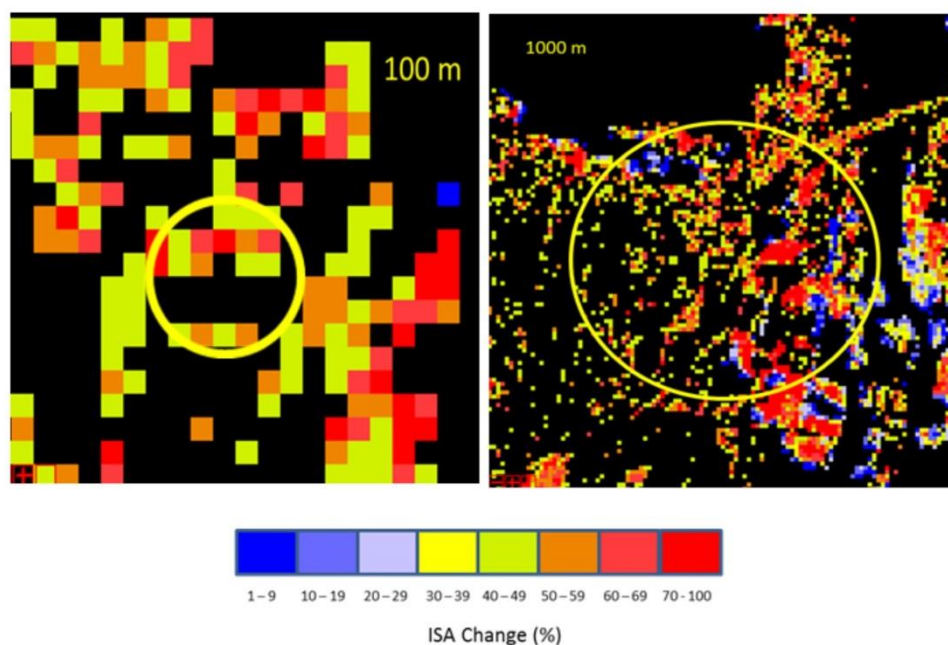
214 Increases in ISA within the 100 and 1000 m radii of each station were characterized by both the
215 percentage increase in ISA from 2001 to 2011 and the percentage of area within the 100 and 1000 m
216 radii associated with the observed increases in ISA. Figure 1 shows an example of the station
217 characterization for change in ISA. The analysis for the USHCN station located at Roseau, MN, indicates
218 that a single 30x30 m grid cell within the 100 m radius exhibited a change in ISA (of 40-49%) between
219 2001 and 2011. This grid cell represents approximately 3% of the area within the 100 m radius of the
220 station location. Thus, the analysis of this station indicates that within the 100 m radius, 3% of the area
221 exhibited a $\geq 10\%$ (as well as $\geq 20\%$) increase in ISA between 2001 and 2011. As only a single grid cell
222 exhibited change within the 100 m radius, none of the area within the 100 m radius exhibited a $\geq 50\%$



223
224 Figure 1. ISA change from 2001 to 2011 for Roseau, MN, USHCN station within 100 (left) and 1000 m
225 radii of station location.
226

227
 228 increase in ISA for this station. A similar analysis for the Roseau, MN station within the 1000 m radius of
 229 the station indicated that 8.2% of the area exhibited a $\geq 10\%$ increase in ISA between 2001 and 2011
 230 while 8% of the area exhibited a $\geq 20\%$ increase. Additionally, within the 1000 m radius, 2.6% of the area
 231 exhibited a $\geq 50\%$ increase in ISA.

232 A second example includes an analysis of the St. George, UT station (Figure 2). The analysis for
 233 this USHCN station indicates that within the 100 m radius 56% of the area exhibited a $\geq 10\%$ (and $\geq 20\%$)
 234



235

236 Figure 2. ISA change from 2001 to 2011 for St. George, UT, USHCN station within 100 (left) and 1000 m
 237 radii of station location.
 238
 239 increase in ISA between 2001 and 2011 while 25% of the area within this radius exhibited a $\geq 50\%$
 240 increase in ISA. Within the 1000 m radius 34% of the area exhibited a $\geq 10\%$ increase in ISA while 32% of

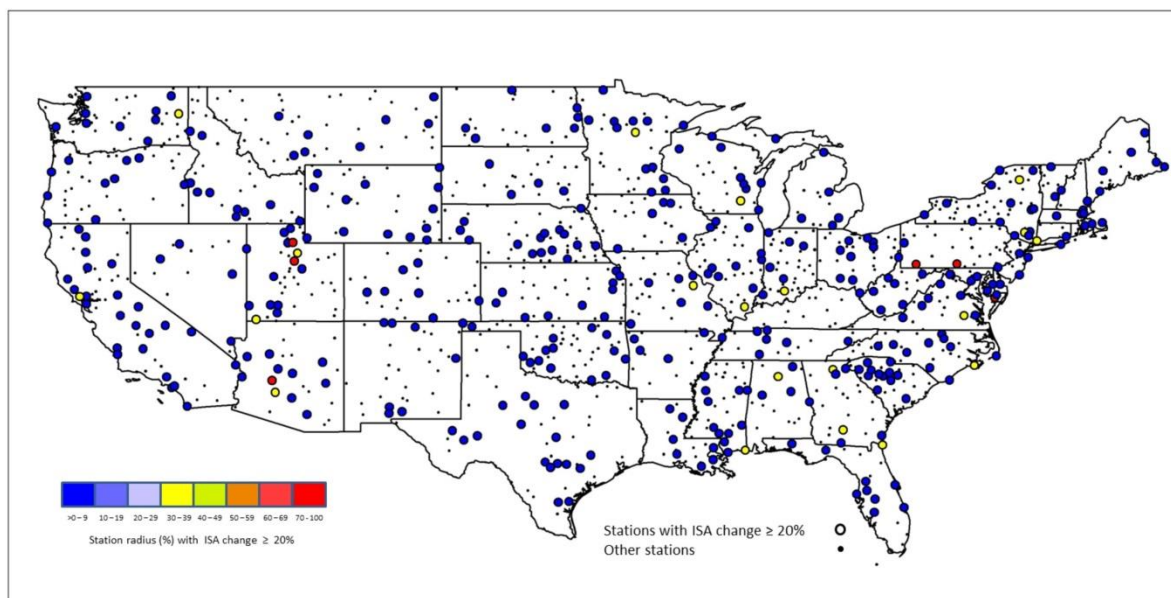
241 the area exhibited a $\geq 20\%$ increase in ISA between 2001 and 2011. Additionally, 19% of the area within
 242 1000 m of the station location exhibited a $\geq 50\%$ increase in ISA.

243

244 3.2 Conterminous US Analysis

245 The spatial distribution of stations that exhibited an increase in ISA of $\geq 20\%$, for any 30 m grid
 246 cell between 2001 and 2011, is displayed in Figure 3 (100 m radius). The total area within the 100 m
 247 radius of each station, that exhibited an increase of $\geq 20\%$, is also indicated for each station location.
 248 Over 32% of the USHCN stations exhibited an increase in ISA of $\geq 20\%$ for at least 1% of the grid cells
 249 within a 100 m radius of the stations (Figure 3). When the 1000 m radius associated with each station
 250 was examined (not shown), over 52% of the stations exhibited an increase in ISA of $\geq 20\%$ within at least
 251 1% of the grid cells within that radius.

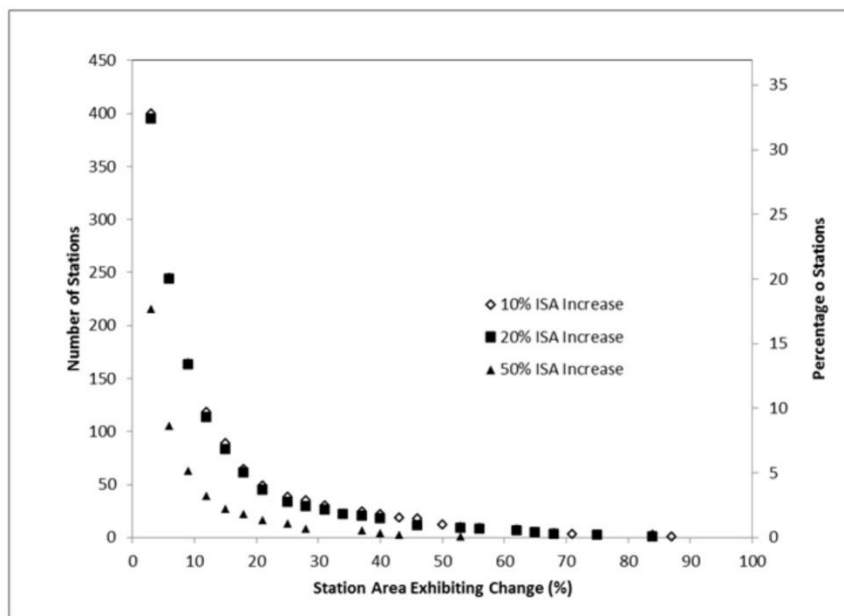
252



253

254 Figure 3. Percentage of area within 100 m radius of USHCN stations that exhibited an increase in ISA of
 255 $\geq 20\%$ between 2001 and 2011. Stations that did not meet this criterion are indicated by black points (.).

256 Figure 4 displays the results of the analysis for changes in ISA within a 100 m radius of 20% or more, as
 257 displayed in Figure 3, but additional analysis for observed increases in ISA of 10 and 50% (as represented
 258 by the different symbols within the figure). For example, an analysis of all 1218 USHCN stations
 259 revealed that 164 stations (left vertical axis) or 13.5% of the stations (right vertical axis) exhibited a \geq
 260 10% increase in ISA for at least 9% (horizontal axis) of the area within a 100 m radius of the stations.
 261 Meanwhile, only 63 stations exhibited a \geq 50% increase in ISA for at least 9% of the area within 100 m of
 262 the stations. Over 32% of the USHCN stations exhibited at least 1% of the grid cells within a 100 m
 263 radius with an increase in ISA of \geq 20% (Figure 4). However, as the required area associated with ISA
 264 change was increased from \geq 1% to \geq 10%, the percentage of stations that were observed with a \geq 20%
 265 increase in ISA between 2001 and 2011 decreased to 9%.



266
 267 Figure 4. Number of stations, and percentage of area within 100 m radius of stations, that exhibits an
 268 increased change in ISA of 10, 20, and 50% between 2001 and 2011. Includes stations with a minimum
 269 of >1% area exhibiting increased ISA.

270

271 Meanwhile, when the 1000 m radius associated with each station was examined, over 52% (over
272 600) of the stations exhibited an increase in ISA of $\geq 20\%$ (Figure 5) within at least 1% of the grid cells.

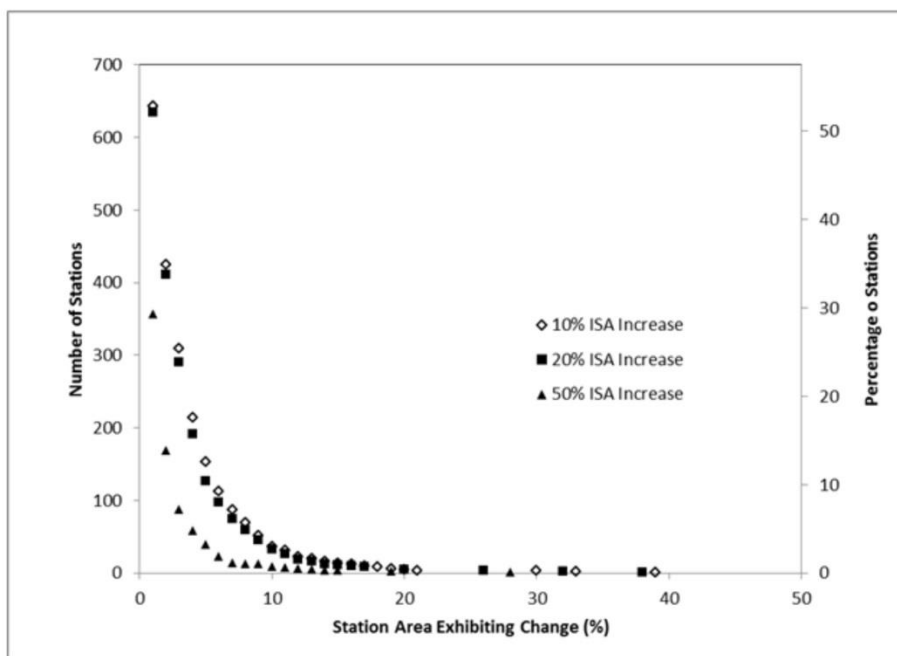
273 However, as the required area associated with ISA change was increased from $\geq 1\%$ to $\geq 10\%$, the number
274 of stations that were observed with a $\geq 20\%$ increase in ISA between 2001 and 2011 decreased to 35

275 (less than 3% of stations). Thus, as the threshold for ISA change increases, e.g., from $\geq 10\%$ to $\geq 50\%$ (as
276 represented by the different symbols), and the area associated with this threshold remains constant,

277 (horizontal axis), the number of stations that exhibit increased ISA (left vertical axis) is decreased

278 (Figures 4 and 5).

279



280

281 Figure 5. Number of stations, and percentage of area within 1000 m radius of stations, that exhibits an

282 increased change in ISA of 10, 20, and 50% between 2001 and 2011. Includes stations with a minimum

283 of $>1\%$ area exhibiting increased ISA.

284

285 Several thresholds of ISA have been used in previous analyses to quantify urbanization of
286 settlements (Imhoff et al 2010, Potere et al 2009, Zhang et al 2010) or climate stations (Hausfather et al
287 2013). Imhoff et al (2010) defined five zones associated with cities included in an analysis of urban heat
288 islands, with a minimum ISA value of 25% used to separate the urban zone from a suburban zone.
289 Potere et al. (2009) utilized an ISA value of 20% to distinguish urban and non-urban areas.
290 ISA was one of four measures of urbanity utilized by Hausfather et al (2013) in an assessment of
291 urbanization on temperature trends of the USHCN stations. ISA was evaluated within a 1 km area
292 surrounding the USHCN station. All of these studies used a single (static) ISA dataset in their analyses,
293 compared to the analysis of change in ISA included within this study.

294 Hausfather et al (2013) identified 357 USHCN stations as urban based on use of a 1000 m grid
295 cell static ISA dataset (nominally 2001) developed from nighttime lights and population data (Elvidge et
296 al 2007). A threshold of 10% ISA was used to distinguish rural ($ISA < 10\%$) and urban ($ISA \geq 10\%$) stations
297 based on the ISA value within the 1000 m grid cell in which the USHCN station was located.

298 The 1000 m analysis of ISA change (2001 to 2011) within this study indicates that as many as
299 1067 stations (87% of stations) exhibited at least one 30 x 30 m grid cell within a 1000 m radius of the
300 station that displayed an ISA change of $\geq 10\%$. When a minimum of 1% of the area within a 1000 m
301 radius of the station location was required to exhibit an ISA change of $\geq 10\%$, 652 stations were observed
302 to meet this criterion. Only 37 stations exhibited an ISA change of $\geq 10\%$ over more than 10% of the area
303 within a 1000 m radius of the station.

304

305

306 **CONCLUSIONS**

307 The availability of gridded impervious surface area (ISA) data presents a consistently measured
308 indicator of a surface feature that may influence the environment near a climate observation station.
309 The level and spatial extent of changes in ISA were evaluated within 100 m and 1000 m buffer radiuses
310 of USHCN stations. Over 32% of the USHCN stations exhibited an increase in ISA of $\geq 20\%$ between 2001
311 and 2011 for at least 1% of the grid cells within a 100 m radius of the station. However, as the required
312 area associated with ISA change was increased from $\geq 1\%$ to $\geq 10\%$, the number of stations that were
313 observed with a $\geq 20\%$ increase in ISA between 2001 and 2011 decreased to 113 (9%). When the 1000 m
314 radius associated with each station was examined, over 52% (over 600) of the stations exhibited an
315 increase in ISA of $\geq 20\%$ within at least 1% of the grid cells within that radius. However, as the required
316 area associated with ISA change was increased to $\geq 10\%$ the number of stations that were observed with
317 a $\geq 20\%$ increase in ISA between 2001 and 2011 decreased to 35 (less than 3% of the stations).

318 The datasets utilized within this study could potentially permit a more detailed spatial
319 assessment of the relative proximity of grid cells with increased ISA to the station locations. Additionally,
320 an assessment of the impact of the spatial distribution of ISA associated with stations on observed
321 temperatures would be recommended. Comparisons of the ISA data with temperature observations
322 should include a thorough assessment of the location of temperature sensors at each station. The
323 availability of increasingly higher resolution remotely sensed data, and the validity of comparisons of
324 this data with in situ observations, will ultimately rely on accurate location information for the data
325 observed by the satellite (or airborne) sensors as well as the ground-based sensors.

326 Minimally, a periodic evaluation of changes in the ISA near the USHCN and other network
327 stations is recommended to assure the local environment around the stations has not significantly
328 changed such that observations at the stations may be impacted.

329

330 **Acknowledgements**

331 The authors acknowledge the assistance of Shelley McNeill and Russell Vose of NOAA's National
332 Centers for Environmental Information (NCEI) with providing detailed USHCN station sensor location
333 information. This manuscript was partially supported by the NOAA/NESDIS Center for Satellite
334 Applications and Research and US Geological Survey. The manuscript contents do not constitute a
335 statement of endorsement, policy, decision, or position on behalf of NOAA or the U.S. Government.

336 **REFERENCES**

337

338 Arnold, C. L., and Gibbons, C. J., 1996. Impervious surface coverage. *American Planning Association*
339 *Journal*, 62, 243-258.

340

341 Christy, J. R., Norris, W. B., and McNider, R. T., 2009. Surface temperature variations in East Africa and
342 possible causes. *J. Climate*, 22, 3342–3356, doi:10.1175/2008JCLI2726.1.

343

344 Christy, J. R., Norris, W. B., Redmond, K. and Gallo, K P, 2006. Methodology and results of calculating
345 central California surface temperature trends: Evidence of human-induced climate change? *J. Climate*,
346 19, 548–563.

347

348 Elvidge, C. D., Tuttle, B. T., Sutton, P. C, Baugh, K. E, Howard A. T., Milesi, C., Bhaduri. B. and Nemani, R.,
349 2007. Global Distribution and Density of Constructed Impervious Surfaces. *Sensors*, 7, 1962-1979.

350

351 Fall, S., Watts, A., Nielsen-Gammon, J., Jones, E., Niyogi, D., Christy, J. R., and Pielke Sr, R. A., 2011.
352 Analysis of the impacts of station exposure on the U.S. Historical Climatology Network temperatures and
353 temperature trends. *J. Geophys. Res.*, 116, D14120, doi:10.1029/2010JD015146.

354

355 Gallo, K. P., Easterling, D. R., and Peterson, T. C., 1996. The influence of land use/land cover on
356 climatological values of the diurnal temperature range. *J. Climate*, 9, 2941–2944.

357

358 Gallo, K., and Xian, G., 2014. Application of spatially gridded temperature and land cover data sets for
359 urban heat island analysis. *Urban Climate* 8, 1–10 doi:10.1016/j.uclim.2014.04.005

360

361 Hale, R. C., Gallo, K.P., Owen, T .W., and Loveland, T. R., 2006. Land use/land cover change effects on
362 temperature trends at U.S. Climate Normals stations. *Geophys. Res. Let.*, 33, L11703, doi:10.1029/
363 2006GL026358.

364

365 Hanamean, J.R. Jr., R.A. Pielke Sr., C.L. Castro, D.S. Ojima, B.C. Reed, and Z. Gao, 2003. Vegetation
366 impacts on maximum and minimum temperatures in northeast Colorado. *Meteorological Applications*,
367 10, 203-215.

368

369 Hausfather, Z., Menne, M. J., Williams, C. N.T., Masters, T., Broberg, R., and Jones, D., 2013.
370 Quantifying the effect of urbanization on U.S. Historical Climatology Network temperature records. *J.*
371 *Geophys. Res. Atmos.*, 118, 481–494, doi:10.1029/2012JD018509.

372

373 Homer, C., Dewitz, J., Yang, L., Jin, S., Danielson, P., Xian, G., Coulston, J., Herold, N., Wickham, J.,
374 Megown, K., 2015. Completion of the 2011 National Land Cover Database for the conterminous United
375 States – Representing a decadal of land cover change information. *Photogrammetric Engineering &*
376 *Remote Sensing*, 81(5), 345-354.

377

378 Imhoff, M. L., Zhang, P., Wolfe, R. E., and Bounoua , L, 2010. Remote sensing of urban heat island effect
379 across biomes in the continental USA. *Remote Sensing of Environment*, 114, 504–513. doi:10.
380 1016/j.rse.2009.10.008.

381

382 Karl, T. R., Diaz, H. F., and Kukla, G, 1988. Urbanization: Its detection and effect in the United States
383 climate record. *J. Climate*, 1, 1099–1123.

384

385 Landsat, 2016. <http://landsat.usgs.gov/> (Accessed on 1 June 2016).

386

387 Leroy M, 2010. Siting classification for surface observing stations on land. In: Proceedings of JMA/WMO
388 workshop on quality management in surface, climate and upper-air observations in RA II(Asia), Tokyo,
389 Japan, 27–23 July 2010, pp 45–64

390

391 Mahmood R, et al., (20+ coauthors), 2010. Impacts of land use land cover change on climate and future
392 research priorities, *Bull. Am. Meteorol. Soc.*, 91, 37–46, doi:10.1175/2009BAMS2769.1.

393

394 NOAA, 2002. Climate Reference Network (CRN) Site Information Handbook. NOAA/NESDIS CRN Series
395 X030.
396 (<http://www1.ncdc.noaa.gov/pub/data/uscrn/documentation/program/X030FullDocumentD0.pdf>)
397 (Accessed on 22 February 2016).

398

399 NOAA, 2016. <http://www.ncdc.noaa.gov/oa/climate/research/ushcn/> (Accessed on 1 June 2016).

400

401 NOAA NCEI, 2016. <http://www.ncdc.noaa.gov/homr/> (Accessed on 31 May 2016).

402

403 Oke T, 2006. Towards better scientific communication in urban climate. *Theor. Appl. Climatol.* 84, 179–
404 190.

405

406 Pielke R. A., Sr, et al. (12+ coauthors), 2007a. Documentation of uncertainties and biases associated with
407 surface temperature measurement sites for climate change assessment. *Bull. Am. Meteorol. Soc.*, 88,
408 913–928, doi:10.1175/BAMS- 88-6-913.

409

410 Pielke, R. A., Sr, et al. (12+ coauthors), 2007b. Unresolved issues with the assessment of multidecadal
411 global land temperature trends. *J. Geophys. Res.*, 112, D24S08, doi:10.1029/2006JD008229.

412

413 Potere, D., Schneide, A., Angel, S., and Civco, D. L., 2009. Mapping urban areas on a global scale.
414 *International Journal of Remote Sensing*, 30(24), 6531-6558.

415

416 Sexton, J.O., Song, X-P, Huang, C., Channan, S., Baker, M.E., Townshend, J.R., 2014. Urban growth of the
417 Washington, D.C.-Baltimore, MD metropolitan region from 1984 to 2010 by annual, Landsat-based
418 estimates of impervious surface, *Remote Sensing of Environment*, 129, 42-53.

419

420 Song, X-P, Sexton, J.O., Huang, C., Channan, S., Townshend, J.R., 2016. Characterizing the magnitude,
421 timing and duration of urban growth from time series of Landsat-based estimates of impervious cover.
422 *Remote Sensing of Environment*, 175, 1-13.

423

424 Story, M. and Congalton, R. G., 1986. Accuracy assessment: A user's perspective. *Photogramm. Engr.*
425 *Remote Sens.*, 32, 397-399.

426

427 USGS, 2014. (<http://www.mrlc.gov/finddata.php>) (Accessed on 17 Dec 2014).

428

429 Wickham, J. D., Stehman, S. V., Gass, L., Dewitz, J., Fry, J. A., and Wade, T. G., 2013. Accuracy
430 assessment of NLCD 2006 land cover and impervious surface. *Remote Sens. Environ.*, 130, 294-304.

431

432 WMO, 2012. Guide to Meteorological Instruments and Methods of Observation. WMO-No. 8, 2008
433 edition Updated in 2010. (http://library.wmo.int/pmb_ged/wmo_8_en-2012.pdf) (Accessed on 22
434 February 2016).

435

436 Xian, G., and Crane, M., 2006. An analysis of urban thermal characteristics and associated land cover in
437 Tampa Bay and Las Vegas using Landsat satellite data. *Remote Sens. Environ.*, 104, 147–156.

438

439 Xian, G., Crane, M., and McMahon, C., 2007. Quantifying multi-temporal urban development
440 characteristics in Las Vegas from Landsat and ASTER Data. *Photogramm. Eng. Remote Sens.* 74 (4), 473–
441 481.

442

443 Xian, G., and Homer, C., 2010. Updating the 2001 National Land Cover Database impervious surface
444 products to 2006 using Landsat imagery change detection methods. *Remote Sensing of Environment*,
445 114 (8):1676-1686.

446

447 Xian, G., Homer, C., Bunde, B., Danielson, P., Dewitz, J., Fry, J., and Pu, R., 2012. Quantifying urban land
448 cover change between 2001 and 2006 in the Gulf of Mexico region. *Geocarto International*, 27, 6, 479-
449 497.

450

451 Xian, G., Homer, C., Dewitz, J., Fry, J., Hossain, N., and J. Wickham, 2011. Change of impervious surface
452 area between 2001 and 2006 in the conterminous United States. *Photogrammetric Engineering &*
453 *Remote Sensing*, 77, 758-762.

454

455 Yuan, F., and Bauer, M. E., 2007. Comparison of impervious surface area and normalized difference
456 vegetation index as indicators of surface urban heat island effects in Landsat imagery. *Remote Sensing of*
457 *Environment*, 106, 375–386.

458

459 Zhang, L., and Weng, Q. 2016. Annual dynamics of impervious surface in the Pearl River Delta, China,
460 from 1988 to 2013, using time series Landsat imagery. *ISPRS Journal of Photogrammetry and Remote*
461 *Sensing*, 113, 86-96.

462

463 Zhang, P., Imhoff, M., Wolfe, R., and Bounoua, L., 2010. Characterizing urban heat islands of global
464 settlements using MODIS and nighttime lights products. *Canadian Journal of Remote Sensing*, 36 (3 Sp.
465 Iss. SI):185-196.

466

467 Zhang, Y., Odeh, I.O.A., and Han, C., 2009. Bi-temporal characterization of land surface temperature in
468 relation to impervious surface area, NDVI and NDBI, using a sub-pixel image analysis.

469 *Int. J. Appl. Earth Obs. Geoinformation*, 11, 256–264.